



# Irradiation behaviour of uranium silicide compounds <sup>☆,☆☆</sup>

M.R. Finlay <sup>a,b,\*,1</sup>, G.L. Hofman <sup>b</sup>, J.L. Snelgrove <sup>b</sup>

<sup>a</sup> Australian Nuclear Science and Technology Organisation, PMB 1, Menai, NSW 2234, Australia

<sup>b</sup> Argonne National Laboratory, 9700 South Cass Avenue, Argonne, IL 60439-4841, USA

Received 11 August 2003; accepted 14 November 2003

## Abstract

A study of the irradiation behaviour of uranium silicide and other related inter-metallic uranium compounds is presented. This study was motivated by the recent discovery that  $U_3Si_2$  undergoes a crystalline to amorphous transformation during irradiation. Such information renders a previously developed fuel swelling model based on the crystalline state of  $U_3Si_2$  invalid. This is of particular significance since low enriched  $U_3Si_2$  dispersion fuels are widely used in research reactors. While such a finding does not alter the well established, stable and benign behaviour of  $U_3Si_2$  during irradiation, it does indicate that a different interpretation of that behaviour is required.

© 2003 Elsevier B.V. All rights reserved.

## 1. Introduction

It is now more than 25 years since the US Government announced its intention to accelerate research into alternative nuclear fuel cycles that did not involve materials usable in nuclear weapons. This ultimately led to a requirement for research reactors to use low enriched uranium, LEU (20%  $^{235}U$ ), rather than high en-

riched uranium, HEU (93%  $^{235}U$ ). Since it was not feasible in most cases to increase fuel loadings, there was a need to find compounds with higher uranium density to compensate for the decrease in uranium enrichment. This fostered vigorous research into the irradiation behaviour of suitable uranium inter-metallic compounds, which offered higher densities than the oxide or aluminide fuels (Table 1). The non-fissile components of these compounds had acceptable neutronic properties, and fuel powder fabrication was relatively simple because of their brittle properties.

Two of the higher density alloys investigated,  $U_3Si$  and  $U_6Fe$  both developed extraordinarily large voids at medium burn-up under irradiation testing that led to unacceptable breakaway swelling. The extremely high growth rates of fission gas bubbles in  $U_3Si$  and  $U_6Fe$  was attributed to fission-induced amorphisation [1]. Such a transformation resulted in changes in fission gas mobility and the plastic flow rate of the fuel that were responsible for the large swelling increases. There was clear independent experimental evidence to support a crystalline to amorphous transformation in those alloys. The bubble morphology of irradiated  $U_3Si$  is shown in Fig. 1. This mechanism was not observed in the lower density  $U_3Si_2$  where a distribution of relatively small and stable fission gas bubbles was observed to form and

<sup>\*</sup> The submitted manuscript has been created by the University of Chicago as Operator of Argonne National Laboratory ('Argonne') under Contract No. W-31-109-ENG-38 with the US Department of Energy. The US Government retains for itself, and others acting on its behalf, a paid-up, non-exclusive, irrevocable worldwide license in said article to reproduce, prepare derivative works, distribute copies to the public, and perform publicly and display publicly, by or on behalf of the Government.

<sup>\*\*</sup> Argonne National Laboratory's work was supported by the US Department of Energy, Office of International Policy and Analysis (NA-241), National Nuclear Security Administration, under Contract No. W-31-109-Eng-38.

<sup>\*</sup> Corresponding author. Address: Argonne National Laboratory, 9700 South Cass Avenue, Argonne, IL 60439-4841, USA.

E-mail address: [rfinlay@anl.gov](mailto:rfinlay@anl.gov) (M.R. Finlay).

<sup>1</sup> On assignment to Argonne National Laboratory.

Table 1  
Density of various fuel meat compounds

Compound	Al	UAl <sub>4</sub>	UAl <sub>3</sub>	UAl <sub>2</sub>	U <sub>3</sub> O <sub>8</sub>	USi	U <sub>3</sub> Si <sub>2</sub>	U <sub>3</sub> Si	U <sub>6</sub> Fe	U
Density g/cm <sup>3</sup>	2.7	5.7	6.8	8.1	8.3	11.0	12.2	15.3	17.4	19.1

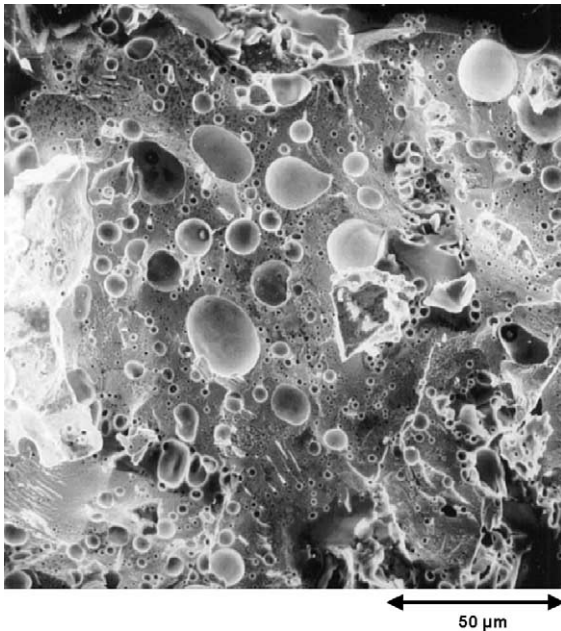


Fig. 1. Fission gas bubble morphology in U<sub>3</sub>Si (73% burn-up,  $4.3 \times 10^{21}$  f/cm<sup>3</sup>).

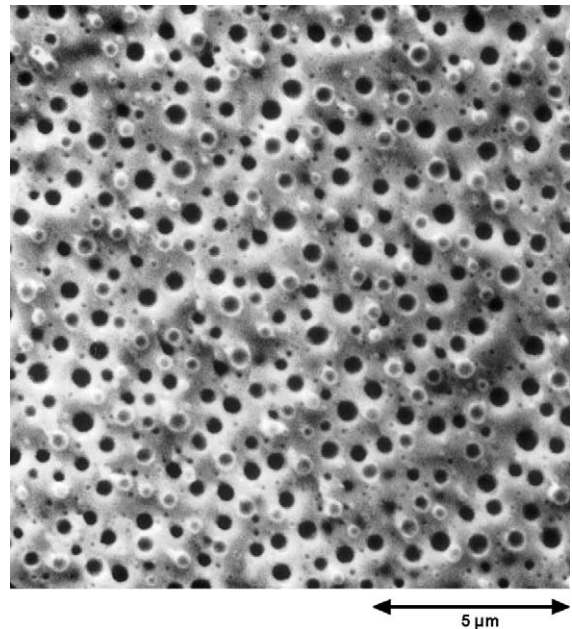


Fig. 2. Fission gas bubble morphology in U<sub>3</sub>Si<sub>2</sub> (96% burn-up,  $5.2 \times 10^{21}$  f/cm<sup>3</sup>).

remain throughout the irradiation to very high burn-up. A detailed SEM micrograph of irradiated U<sub>3</sub>Si<sub>2</sub> is shown in Fig. 2.

On the basis of the fission gas behaviour in U<sub>3</sub>Si<sub>2</sub> and the absence of any clear contradictory evidence it was concluded that U<sub>3</sub>Si<sub>2</sub> was a crystalline material. An irradiation-induced recrystallisation model of fission gas behaviour was developed to explain the stable swelling behaviour [2]. Similar observations had been made in ceramic fuels, such as UO<sub>2</sub> [3]. However, more recent work has revealed that the U<sub>3</sub>Si<sub>2</sub> becomes amorphous almost instantaneously upon irradiation [4].

In the current work, a review of the mini-plates irradiated in the Oak Ridge research reactor (ORR) from the U<sub>3</sub>Si<sub>2</sub> qualification program was made. The aim is to provide a description of the irradiation behaviour of amorphous U<sub>3</sub>Si<sub>2</sub> in sufficient detail to allow modelling under irradiation [5]. Much of the detailed analytical work performed previously on U<sub>3</sub>Si<sub>2</sub> fuel samples was aimed to elucidate the demonstrated stability of the fuel at high burn-up. In this work, the primary focus was on the lower burn-up mini-plates as the fission gas bubble morphology evolved. The present

study has focused on bubble nucleation, growth and morphology and monitored changes in bubble number and composition as a function of fission density. This paper reports a new understanding of U<sub>3</sub>Si<sub>2</sub> behaviour under irradiation.

## 2. Crystalline to amorphous transformation

It was widely recognised that U<sub>3</sub>Si becomes amorphous when irradiated as reported by Bleiberg [6], Bloch [7] and Bethune [8]. It had also been demonstrated that the behaviour of fission gas bubbles in U<sub>3</sub>Si and U<sub>3</sub>Si<sub>2</sub> was significantly different [9]. Given those differences and the absence of any contradictory information it was concluded that U<sub>3</sub>Si<sub>2</sub> remained crystalline during irradiation.

Very low levels of swelling in U<sub>3</sub>Si<sub>2</sub>, even at high burn-ups was attributed to a uniform bimodal distribution of fission gas bubbles which showed no signs of coalescence. Those observations suggested that an underlying microstructure was responsible for the behaviour. An irradiation-induced recrystallisation

model was developed that relied on the presence of sufficient grain boundary surface to trap and pin fission gas bubbles and prevent coalescence [2].

The model was fully developed and then incorporated into the DART code (dispersion analysis research tool) [10]. DART is a mechanistic model for the prediction of fission product-induced swelling in dispersion fuels. DART calculates the irradiation-induced fission gas bubble size distributions as a function of fuel morphology, as well as solid fission product swelling. Fission gas bubbles were considered to nucleate at approximately the time of grain recrystallisation and remain relatively constant in number throughout the irradiation. The larger bubbles were believed to be associated with grain boundary junctions and the smaller bubbles were located on grain boundary surfaces.

Subsequently, electron diffraction analysis of Kr ion irradiation tests on  $U_3Si_2$  foils and more comprehensive neutron diffraction studies [4] demonstrated that  $U_3Si_2$  becomes amorphous under irradiation. The individual Kr ions and the energetic fragments from the uranium fissions produce tracks of damage in the form of amorphous zones. The amorphous volume fraction increases rapidly and complete amorphisation occurs at a dose of approximately  $1.1 \times 10^{20}$  f/cm<sup>3</sup>. Interestingly, the unit cell volume decreases linearly with increased volume fraction of amorphous material. Conversely,  $U_3Si$  swells grossly on amorphisation and the large free volume produced permits more rapid migration of fission gas atoms and bubbles than compared to  $U_3Si_2$ .

Consequently, the recrystallisation model does not adequately explain the nucleation and growth of fission gas bubbles in  $U_3Si_2$ . Whilst it appears to work well within the range of measured data, it is fundamentally flawed and cannot be relied on to extrapolate beyond that range.

### 3. Irradiation test program

The irradiation testing program of uranium intermetallic compounds was conducted by the Reduced Enrichment for Research and Test Reactors (RERTR) program. A comprehensive program of mini-plate irradiations was performed to evaluate different compounds and develop an understanding of their irradiation behaviour. In all, more than 200 mini-plate irradiations were performed in the ORR from July 1980 to January 1987, including, but not limited to  $U_3Si$ ,  $U_3SiAl$ ,  $U_3Si_2$ ,  $USi$ ,  $U_6Fe$  and  $U_6Mn$  cores. The mini-plates measured  $50 \times 114 \times 1.27$  or  $1.52$  mm and consisted of a core of fuel powder dispersed in pure aluminium, with aluminium alloy 6061 picture frame and cladding.

The irradiation performance of each fuel was evaluated by the fuel plate volume increase and post-irradiation microstructural examination. The  $U_6Fe$  [11] and

$U_6Mn$  [12] mini-plates exhibited unacceptable swelling behaviour during irradiation testing. Extensive and inter-linked fission gas bubbles resulted in failure by pillowing at relatively low fission densities.

The mini-plate irradiations of uranium silicide compounds consisted of two phases and are reported in detail by Senn [13], and Snelgrove et al. [14]. The initial program was designed to evaluate the primary candidates and included four  $U_3Si_2$ , 18  $U_3Si$  and 36  $U_3SiAl$  mini-plates. The second program of more extensive tests on the selected fuels included 10  $USi$ , 35  $U_3Si_2$  and 34  $U_3Si$  mini-plates. Variations in fuel volume loading and enrichment levels were incorporated to determine failure thresholds.

## 4. Irradiation swelling behaviour

### 4.1. $U_3Si$

$U_3Si$  was the preferred candidate because it offered the highest uranium density of the uranium silicide compounds. Fig. 3 shows that the swelling behaviour was not dissimilar to that of  $U_6Fe$ ,  $U_6Mn$  or  $U_3SiAl$ . The very high density candidates all exhibited unacceptable swelling rates at low and medium fission densities. The lower density compounds of  $U_3Si_2$  and  $USi$

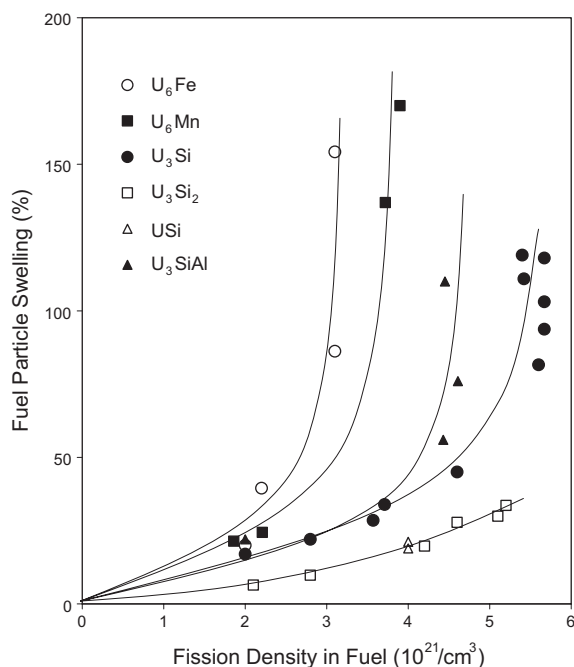


Fig. 3. Fuel particle swelling ( $\Delta V_f$ ) as a function of fission density. The fuel particle swelling is calculated from the mini-plate swelling.

Table 2  
Enthalpy of formation of various uranium compounds

Compound	U <sub>3</sub> Si <sub>2</sub>	USi	U <sub>3</sub> Si	U <sub>6</sub> Mn	U <sub>6</sub> Fe
$\Delta H_f$ kJ mol <sup>-1</sup>	-167	-84	-80	-88	-17

exhibited swelling rates which were greatly reduced compared to the higher density fuels and are regarded as stable and acceptable.

The fuel particle fracture surface of U<sub>3</sub>Si (Fig. 1) illustrates a much higher mobility of fission gas compared to U<sub>3</sub>Si<sub>2</sub>. The fission gas bubbles exhibit a non-uniform distribution of varying shapes and sizes and show signs of migration and inter-linkage. The swelling behaviour is determined by the stability of each compound under irradiation. It has been proposed that irradiation-enhanced diffusion and plastic flow of the fuel controls the fission gas bubble growth [15], and ultimately the onset of the breakaway swelling.

Those compounds which offer the highest uranium density also tend to be the most unstable, including U<sub>6</sub>Fe, U<sub>6</sub>Mn, and U<sub>3</sub>Si. Generally these alloys tend to form by a peritectoid reaction from two-phase mixtures at relatively low temperatures and are less thermodynamically stable compared to U<sub>3</sub>Si<sub>2</sub> and USi, which melt congruently at much higher temperatures. The enthalpies of formation for relevant uranium compounds are listed in Table 2.

#### 4.2. U<sub>3</sub>Si<sub>2</sub>

The remarkable difference between U<sub>3</sub>Si<sub>2</sub> and U<sub>3</sub>Si was not only reflected in the irradiation swelling behaviour but also in fission gas bubble morphology as shown by Fig. 2. In the stable compounds such as U<sub>3</sub>Si<sub>2</sub>, the fission gas bubble morphology is uniform with no clear evidence of bubble coalescence or inter-linkage. The small fission gas bubbles remain stable to high burn-up. Even at 63% burn-up of a 93% enriched HEU mini-plate, the fission gas bubbles retain a uniform morphology, as shown in Fig. 4.

Fig. 5 shows the swelling data of U<sub>3</sub>Si<sub>2</sub> fuel particles as a function of fission density. The data points were measured; the lines were an interpretation of the swelling behaviour made at the time the data were analysed [9]. The current knowledge of amorphisation of U<sub>3</sub>Si<sub>2</sub> under irradiation has altered the interpretation of the swelling data. A new and refined understanding of the swelling behaviour of U<sub>3</sub>Si<sub>2</sub> is presented in Section 6.

Nonetheless, two very important observations were made that still underpin current understanding of the swelling behaviour. Firstly, the initial rate of swelling is relatively low, and then accelerates markedly. This transition referred to as the 'knee point' marks the fission density at which the fission gas bubbles reach a sufficient size to influence swelling behaviour in addition

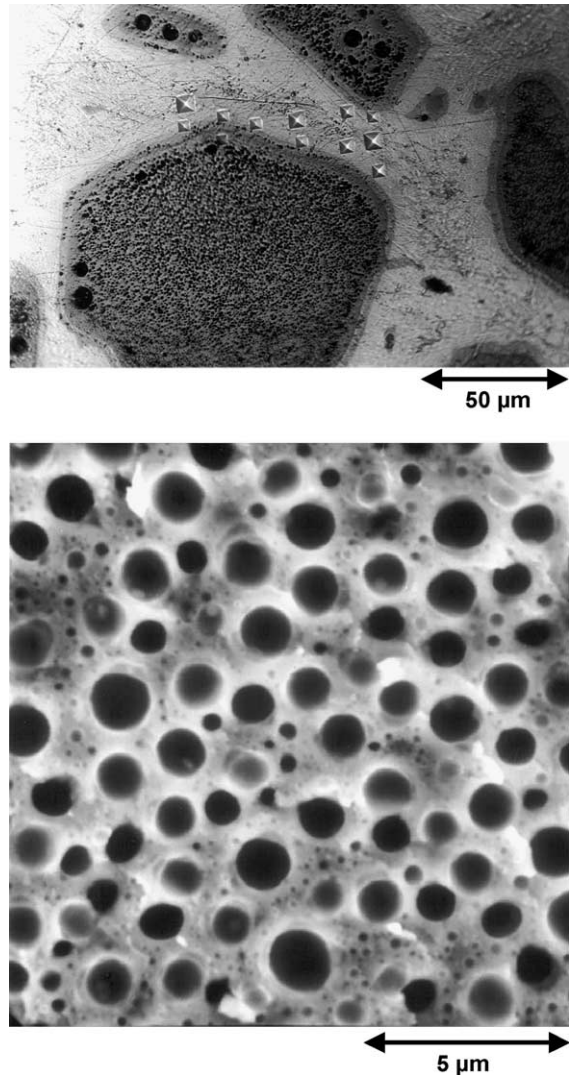


Fig. 4. Optical and scanning electron micrographs of an HEU fuel particle at a fission density of  $14.3 \times 10^{21}$  f/cm<sup>3</sup>.

to solid fission products. Prior to the knee, a small fraction of the fission gas is retained in solution while the rest is believed to be stored in nanometre-size bubbles which are below the limit of resolution of the SEM. Secondly, the fission rate appeared to influence the fission density at which the fuel swelling began to accelerate. At a higher fission rate the knee point is shifted to a higher fission density.

#### 4.3. USi

Based on the limited data available, it appeared as though the USi mini-plates exhibited irradiation

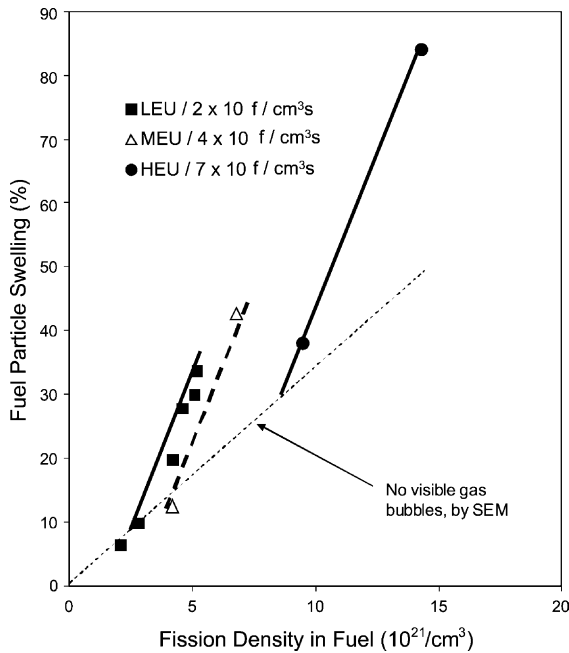


Fig. 5. Interpretation of  $\text{U}_3\text{Si}_2$  fuel particle swelling at different fission rates. The fission rates indicated were averaged over the irradiation period [9].

swelling behaviour similar to  $\text{U}_3\text{Si}_2$ . The lower density of USi means that the uranium is almost fully fissioned at moderately high fission densities, and hence, it is not possible to determine whether the swelling behaviour would diverge from the  $\text{U}_3\text{Si}_2$  at higher fission density. The bubble morphology shown in Fig. 6 is uniform and appears to be similar to that of  $\text{U}_3\text{Si}_2$ . Analysis of the bubble density however, shows that there are fewer bubbles than for comparable  $\text{U}_3\text{Si}_2$  mini-plates, that the bubbles are larger and that the inter-bubble spacing is greater. This suggests that fission gas mobility is higher in USi than  $\text{U}_3\text{Si}_2$ . It is not however, as high as for the  $\text{U}_3\text{Si}$  where the fission gas bubbles show no uniformity. Predictions of fission gas stability have been related to the thermodynamic properties of each compound [15]. In this case the enthalpy of formation of both  $\text{U}_3\text{Si}$  and USi are very similar (Table 2) and hence cannot independently provide an explanation for the difference in behaviour. There are no published data on the behaviour of USi during a crystalline to amorphous transformation. Given the known behaviour of the other silicide compounds during such a transformation, changes in the unit cell dimension may account for the mobility of fission gas atoms. Given the higher uranium density and superior performance of the  $\text{U}_3\text{Si}_2$ , no further effort was made to pursue USi.

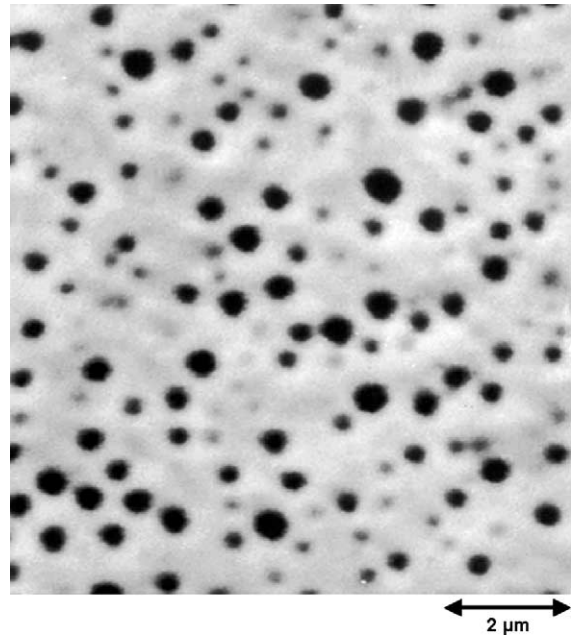


Fig. 6. Fission gas bubble morphology in USi (87% burn-up,  $4.1 \times 10^{21} \text{ f/cm}^3$ ).

#### 4.4. $\text{U}_3\text{SiAl}$

$\text{U}_3\text{SiAl}$  (3.5wt% Si, 1.5wt% Al) was originally expected to be the most suitable low enriched fuel, based on experience gained in the Canadian Reactor Program [16] and the lack of data on  $\text{U}_3\text{Si}$  and  $\text{U}_3\text{Si}_2$ . Aluminium was added to  $\text{U}_3\text{Si}$  to improve corrosion resistance. The fuel however, proved to be the least attractive of the three silicide compounds, as shown in Fig. 3. The swelling of  $\text{U}_3\text{SiAl}$  is inferior to the  $\text{U}_3\text{Si}$  and  $\text{U}_3\text{Si}_2$  and was found to have failed by pillowing at 75% burn-up ( $2.2 \times 10^{21} \text{ f/cm}^3$ ).

Fig. 7 illustrates the difference in fission gas behaviour between  $\text{U}_3\text{Si-Al}$ ,  $\text{U}_3\text{Si}$  and  $\text{U}_3\text{Si}_2$  under the same irradiation conditions. The  $\text{U}_3\text{SiAl}$  fuel is in the advanced stages of breakaway swelling. Individual fuel particles have merged into a globular mass which is dominated by the linking up of large fission gas bubbles. The continued linkage of the larger bubbles eventually resulted in plate failure by pillowing. In the  $\text{U}_3\text{Si}$  fuel, the fuel particles have lost their original angular shape and appear to be linking together. Fission gas bubbles are clearly evident and the first sign of inter-linking is present; however, there has been little growth relative to the  $\text{U}_3\text{SiAl}$ . In the  $\text{U}_3\text{Si}_2$  fuel, the fission gas bubbles are too small to be resolved by optical microscopy. The fuel particles have retained their angular shape and show few signs of inter-linking.

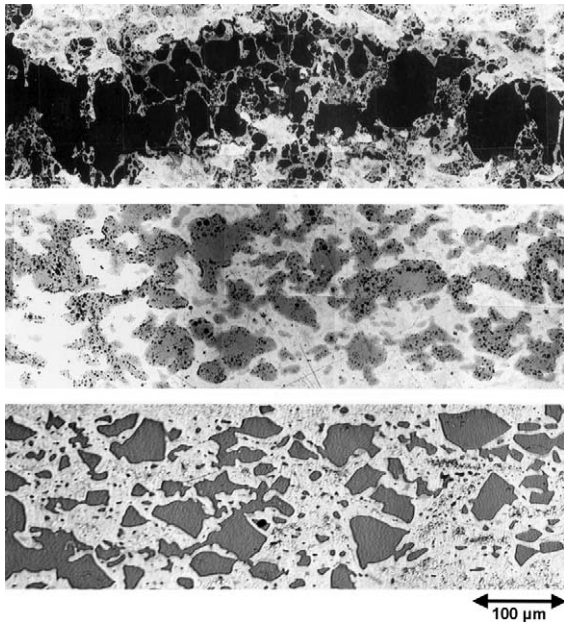


Fig. 7. Post irradiation optical micrographs showing fuel meat microstructure of as-polished  $U_3Si-Al$ ,  $U_3Si$  and  $U_3Si_2$  after 96% burn-up.

Aluminium has a deleterious effect on the swelling behaviour of uranium silicide compounds. The substitution of silicon with aluminium appears to increase the mobility of fission gas atoms. Whilst  $U_3SiAl$  demonstrates most effectively the effect of aluminium, the  $U_3Si$  illustrates the effect of a smaller quantity of aluminium. Fission gas bubble growth has occurred predominantly at the periphery of the fuel particles. The aluminium has diffused from the dispersion matrix and increases gas mobility in that area. A similar effect was observed in the high burn-up HEU  $U_3Si_2$  mini-plate (Fig. 4).

#### 4.5. $U_3SiCu$

Once the irradiation results showed that  $U_3SiAl$  was prone to breakaway swelling there was a shift in emphasis toward  $U_3Si$  and  $U_3Si_2$  fuels. Although aluminium was shown to reduce the stability of  $U_3Si$ , copper was considered to have the potential to increase it. Aluminium was believed to reduce the stability of  $U_3Si$  because of its low binding energy with vacancies in the matrix [1]. Conversely, copper was generally known to have higher binding energies with vacancies. A small number of  $U_3Si$  mini-plates were irradiated that contained  $\sim 1.7$ wt% copper. Fig. 8 indicates that there is no apparent benefit in the case of the LEU  $U_3SiCu$  mini-plates (volume fraction of the fuel phase was approximately 45%) since the swelling data is not distinguishable from the  $U_3Si$  data. However, the medium

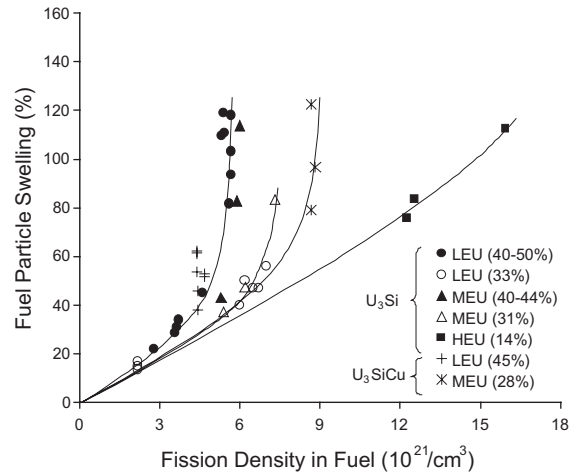


Fig. 8. Swelling of  $U_3Si$  and  $U_3SiCu$  fuel particles. The volume fraction of fuel particles is indicated in the legend.

enriched uranium (MEU)  $U_3SiCu$  mini-plates indicate that the onset of breakaway swelling shifted to a higher fission density compared to  $U_3Si$ , indicating that copper has induced some positive effect. It was not possible to make a comprehensive assessment however, as there was insufficient irradiation data. No further effort was made to pursue additions of copper, as there was no demonstrated benefit for the LEU  $U_3SiCu$ .

#### 4.6. Fuel loading

In  $U_3Si_2$ , practical fuel plate fabrication considerations [14] limit the volume fraction of fuel that can be added to the dispersant, aluminium. The current limits for  $U_3Si_2$  lie between 40% and 45% volume fraction, to yield a uranium density of  $4.8 \text{ g/cm}^3$ , as approved by the US Nuclear Regulatory Commission [17]. Fuel particle swelling in  $U_3Si_2$  is low due to the stable, non-interacting sub-micron sized fission gas bubbles and is unaffected by fuel volume fraction. However, for less stable fuels, such as  $U_3Si$ ,  $U_3SiAl$ , and  $U_6Fe$ , a larger fuel volume fraction can increase the amount of swelling that occurs. This is illustrated by the different loadings of  $U_3Si$  mini-plates in Fig. 8. An increased level of aluminium in the matrix increases the separation between fuel particles and delays the inter-linkage of fuel particles that leads to breakaway swelling. The aluminium also provides mechanical restraint against the rapidly expanding fuel particles. The mechanical restraint provided by cylindrical cladding allows the less stable  $U_3Si$  to be utilised for certain rod type fuel [18]. A more highly loaded plate will undergo accelerated swelling at a lower fission density compared to a plate with a lower volume fraction of fuel.

## 5. Analysis of $U_3Si_2$ fuel swelling

### 5.1. Fission gas bubble distribution

A detailed analysis of the bubble size distribution of a selected number of  $U_3Si_2$  mini-plates yielded new information that is not consistent with previous findings [10]. The two major differences are (a) the number of fission gas bubbles was not constant throughout the irradiation period, and (b) the bimodal distribution of fission gas bubbles was not observed until well after the knee point. These observations contradict two fundamental points that form the basis of the fuel swelling model of  $U_3Si_2$  in a crystalline state.

The bubble distributions were measured manually, from micrographs of fracture surfaces and converted to a volumetric fraction using the Saltykov method [19]. At the fission density where bubbles were first observed, the distribution of bubble sizes was narrow and the number of bubbles at the peak size was high (Fig. 9). This point, as already explained is referred to as the knee. Mini-plates that were irradiated to higher burn-up showed that the distribution of bubble sizes broadened as the bubbles accumulated more fission gas.

If the bubbles had grown at a constant rate, the distribution would have remained relatively uniform over all fission densities. However, the distribution evolved in a non-uniform manner, as shown in Fig. 9. The total number of bubbles decreased as a function of fission density; some of the bubbles grew at a preferential rate and this suggested that bubble coalescence or re-resolution had occurred. The strong influence of the fission rate, as explained in Section 5.3, probably influences bubble nucleation at the knee and hence comparison between mini-plates of considerably different fission rate history is not necessarily valid. Three mini-plates identified in Fig. 10 as A224, A92 and A93 were irradiated with very similar fission rate histories. The irradiation of A224 was stopped at a fission density of  $2.8 \times 10^{21}$  f/cm<sup>3</sup>; the irradiations of A92 and A93 were

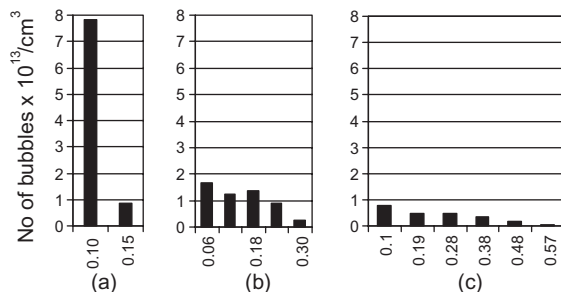


Fig. 9. Number and distribution of fission gas bubbles ( $\mu\text{m}$ ) at fission densities of (a)  $2.8 \times 10^{21}/\text{cm}^3$ , (b)  $4.2 \times 10^{21}/\text{cm}^3$ , and (c)  $4.6 \times 10^{21}/\text{cm}^3$ .

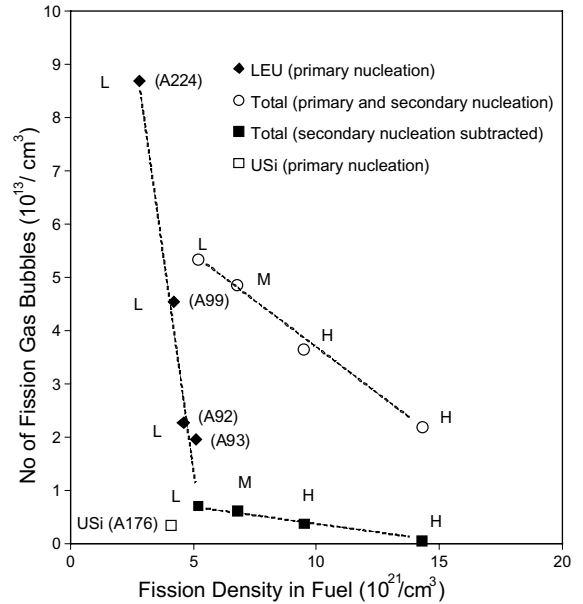


Fig. 10. Number of bubbles per cm<sup>3</sup> in irradiated  $U_3Si_2$  fuel particles. L = LEU, M = MEU, H = HEU.

continued to  $4.6 \times 10^{21}$  f/cm<sup>3</sup> and  $5.1 \times 10^{21}$  f/cm<sup>3</sup>, respectively. Despite a similar irradiation history, the numbers of bubbles measured for A92 and A93 were lower than for A224 by a factor of four. This provides evidence that fission gas bubbles decrease in number as a function of fission density, either through coalescence or re-resolution.

This observation was difficult to reconcile with the bubble morphology. Generally, the bubbles were uniformly dispersed throughout the fuel particles with little evidence of coalescence or bubbles situated adjacent to one another. However, calculations indicate that the bubbles disappeared at a rate of only  $\sim 1$  bubble every 2–3 min, per 1000  $\mu\text{m}^3$ . Given that each SEM micrograph examined represented a single cross section through such a volume it was not so surprising that little evidence for coalescence was found.

It was also apparent that the visible bubbles did not follow a bimodal distribution. The bimodal distribution of fission gas bubbles was not observed until very high burn-up was achieved (Fig. 11). A sibling mini-plate that had been irradiated under the same irradiation conditions (same module) but removed at a fission density of  $4.8 \times 10^{21}$  f/cm<sup>3</sup> showed no evidence of an emerging second population of fission gas bubbles. This indicates that a secondary nucleation of bubbles occurred at a point well after the primary nucleation of bubbles. After the nucleation of another generation of small bubbles, the number of visible bubbles from the primary nucleation continued to decrease, although at a slower rate.

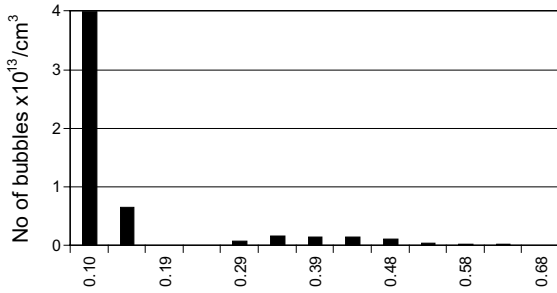


Fig. 11. Number and distribution of fission gas bubbles ( $\mu\text{m}$ ) at a fission density of  $5.2 \times 10^{21}/\text{cm}^3$ .

### 5.2. Fission gas bubble composition

The number of fission gas atoms stored in bubbles was calculated and compared against the total number of atoms generated. The results are plotted in Fig. 12 and reveal two surprising features of fission gas bubbles. Firstly, the percentage of gas atoms stored in bubbles was very small. Secondly, the higher enrichment fuels, that is, MEU and HEU, that generate a larger number of fission gas atoms, store a smaller fraction of the gas generated in those bubbles. Although it is known that the larger bubbles are under less pressure than the smaller bubbles, the increased volume was expected to compensate for the pressure differential. The bubbles in an irradiated HEU  $\text{U}_3\text{Si}_2$  fuel that had a bubble volume fraction of 68% (Fig. 4) only contained between 5% and 20% of the total gas atoms generated. The surface

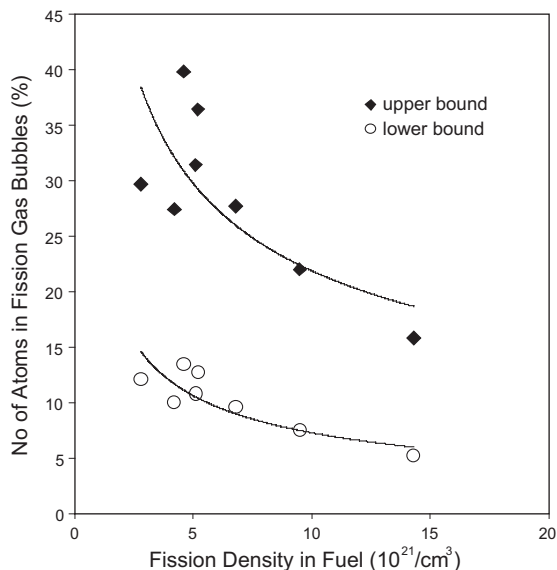


Fig. 12. Number of fission gas atoms in bubbles as a percentage of the total number of fission gas atoms generated.

energies of fission gas bubbles are not well known for common nuclear fuels such as  $\text{UO}_2$  and, therefore, are even less understood for amorphous alloy fuels. Hence, an upper and lower bound value was used in calculations.

### 5.3. Fission rate effect

The nucleation of fission gas bubbles is a complex phenomenon that is not well-understood in amorphous materials. It is related to the ability of the material to store fission gas in solution and/or nanometre-sized bubbles. At the knee point, the swelling rate of the fuel particle accelerates as observable fission gas bubbles are nucleated. Hofman et al. [9] demonstrated that the higher fission rate of the MEU and HEU fuels shifted the knee to a higher fission density compared to the lower fission rate of the LEU fuels. At a higher fission rate, more fission fragment-gas atom collisions occur that provide the energy to retain the fission gas atoms in solution.

Although the fission rate dependence of the knee position was recognised, the fuels were grouped according to enrichment and an average fission rate was applied to each group. The swelling curves beyond the knee were determined as linear fits of the data for the three general fission rates experienced in the LEU, MEU and HEU mini-plates, as illustrated in Fig. 5. The detailed fission rate histories of a number of mini-plates are shown in Fig. 13.

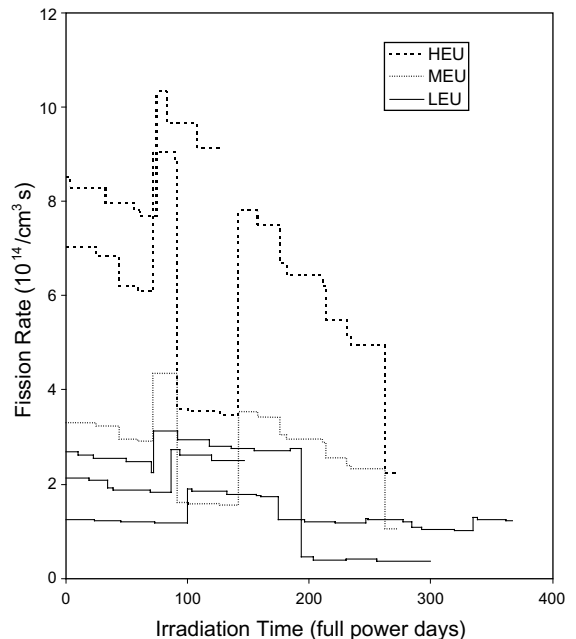


Fig. 13. Fission rate history of various  $\text{U}_3\text{Si}_2$  mini-plates irradiated in the Oak Ridge research reactor.



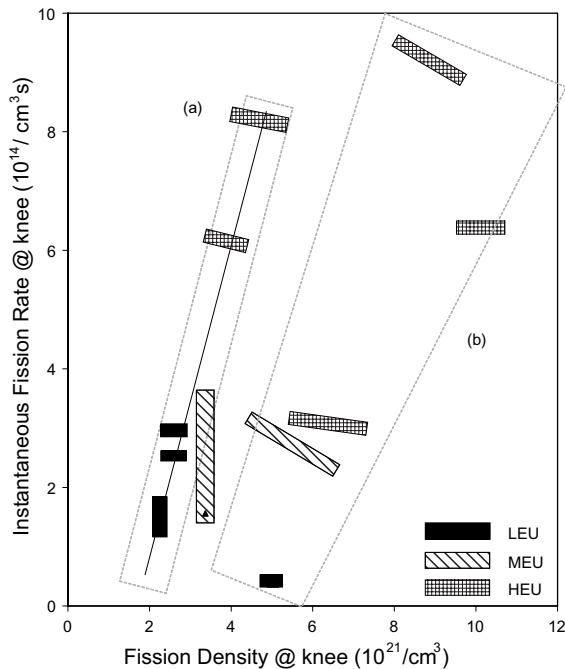


Fig. 14. Fission rate dependence of the knee or point of (a) primary nucleation, and (b) secondary nucleation of fission gas bubbles.

The individual fission rate history of each mini-plate is a function of the instantaneous burn-up of the fuel and vertical location of the irradiation modules, which sometimes were relocated between cycles. It is highly likely that the fission rate history influenced the position of the knee. From a review of the fission rate histories, a correlation has been developed that relates the fission density at the knee to the instantaneous fission rate at the knee. The correlation has been bounded by a window to reflect the uncertainty in identifying the knee. A similar effort has been made for the secondary nucleation but the lack of data means that the uncertainty is considerably higher. The correlation, shown in Fig. 14, indicates that a higher instantaneous fission rate shifts the knee to a higher fission density. It is important to recognise that the behaviour of the fission gas will vary according to the fission rate at that time, and not an average fission rate. Therefore, the fission gas solubility is believed to be fission rate dependent. If the instantaneous fission rate is above a threshold value, the fission gas will be retained in solution and no bubbles should appear. If the instantaneous fission rate is at or below the threshold, then bubbles should appear.

#### 5.4. Chemistry effect on fission gas solubility

Fig. 15 illustrates the amount of gas in bubbles and in solution and the corresponding total amount of gas for a

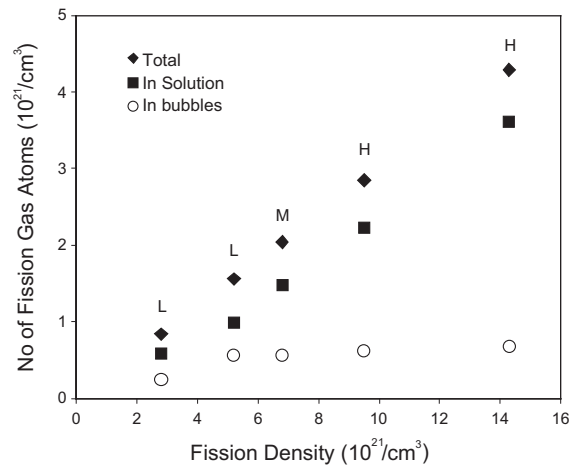


Fig. 15. Fission gas atom behaviour as a function of fission density.

series of mini-plates. A close inspection of the two LEU mini-plates reveals that the amount of fission gas in solution has increased between the mini-plate at the knee point and the mini-plate at the point of secondary nucleation. On the basis of the explanation above, the fission rate would be expected to have increased to cause more gas atoms to be in solution. Despite the step changes in fission rate, illustrated in Fig. 13, the general trend is for the fission rate of each mini-plate to decrease as a function of fission density. Therefore, this observation is not consistent with the fission rate effect and indicated that another factor influences the behaviour of fission gas in solution.

It is proposed that the changing chemistry influences the diffusivity of fission gas atoms in solution. As the uranium is consumed, the ratio of uranium to silicon atoms decreases. A considerable quantity of fission product elements are also accumulated but their effect on the chemical state of the fuel is too complex to address here. This paper will focus on the primary change in the uranium to silicon ratio. Fig. 16 illustrates how the uranium-to-silicon ratio changes as a function of fission density. The silicon-to-silicon bonds, which are stronger than the uranium-silicon bonds, probably reduce the diffusivity of fission gas atoms in solution. Therefore, migration of fission gas atoms to fission gas bubbles becomes more difficult and as a result, more fission gas is stored in solution. This effectively increases the solubility limit, which continually changes, and is influenced by the uranium-to-silicon ratio and the fission rate. Fission gas is produced, however, at a faster rate than the increasing solubility limit can accommodate, and at some point a secondary nucleation of fission gas bubbles occurs.

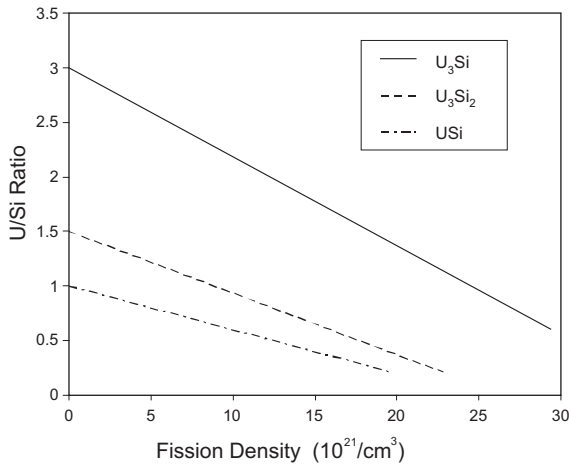


Fig. 16. Change in the uranium-to-silicon ratio vs. fission density as 93% enriched U<sub>3</sub>Si, U<sub>3</sub>Si<sub>2</sub> and USi is burned.

The strongest evidence to support this proposal is found in the behaviour of fission gas in USi fuel. The ratio of silicon to uranium is higher in USi than in U<sub>3</sub>Si<sub>2</sub> fuel. Comparisons between U<sub>3</sub>Si<sub>2</sub> and USi mini-plates irradiated to an equivalent fission density reveal significant differences in fission gas bubble number as shown in Fig. 10. Fission product generation is expected to be similar in both fuels and hence the silicon content is the primary difference between the two irradiated fuels. The number of fission gas bubbles measured in A99 (U<sub>3</sub>Si<sub>2</sub>) was an order of magnitude greater than for A176 (USi). The smaller number of fission gas bubbles in the USi indicates that a larger quantity of gas is stored in solution. Further evidence for this hypothesis has been found in the growth of the interaction layer between the fuel particle surface and the aluminium matrix. Hofman et al. [20] derived a correlation for the growth of the interaction layer for LEU U<sub>3</sub>Si<sub>2</sub> fuels but were unable to apply it to the MEU and HEU U<sub>3</sub>Si<sub>2</sub> fuels or the LEU and MEU USi fuels. The rate of growth in those fuels was too low to fit the correlation. It is considered that the increased silicon-to-uranium ratio of those fuels reduced the diffusivity of aluminium in much the same way that it is believed to affect the diffusivity of fission gas atoms in solution. An out of pile experiment conducted by DeLuca et al. [21] added silicon to uranium–aluminium diffusion couples demonstrated a reduction in the growth of the reaction layer by a factor of at least three between 325 and 550 °C.

## 6. Fuel swelling behaviour

A new interpretation of the fuel swelling behaviour of U<sub>3</sub>Si<sub>2</sub> fuel is shown in Fig. 17. Although it draws from

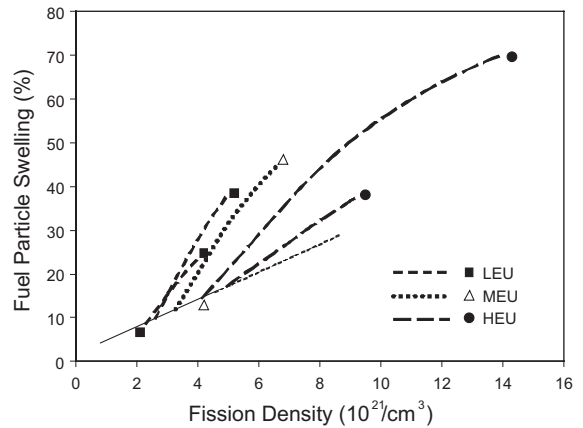


Fig. 17. Proposed swelling behaviour of U<sub>3</sub>Si<sub>2</sub> fuel particles from selected mini-plates.

the observations reported above, it is still largely based on the original fuel swelling model proposed by Rest and Hofman [10]. It differs from the previous interpretation in two ways. Firstly, the position of the knee is not determined by a general fission rate, but is based on an individual fission rate history according to the correlation shown in Fig. 14. As a result the knee point may vary between mini-plates of the same nominal enrichment because fission rate is not solely a function of the enrichment, but also the in-core position. Secondly, the swelling curve of each mini-plate has been illustrated as non-linear. This is particularly evident for the HEU mini-plate, given the large change in the uranium-to-silicon ratio. As the uranium-to-silicon ratio decreases and the proportion of gas in the fission gas bubbles continues to decrease, the swelling rate is also expected to decrease. Since there is only one data point per mini-plate, the shape of the swelling curves are estimated, based on the arguments presented in Section 5.3.

The fission rate effect and the changing uranium-to-silicon ratio both influence bubble behaviour and ultimately fuel particle swelling. It is difficult to separate the two effects and identify their individual influence. The fission rate effect is likely to dominate at the lower fission densities when the change in the uranium-to-silicon is small. However, at the higher fission densities, particularly the MEU and HEU fuels, the change in the uranium-to-silicon ratio is significant and expected to exert a strong influence. This is reflected in the decrease in the rate of swelling shown for the HEU mini-plates.

The various fission products almost certainly affect the fission gas solubility and also the surface energy which influences fission gas bubble size. However, these appear to be indeterminable at this time and are ignored in this study.

## 7. Conclusion

The irradiation behaviour of uranium silicide compounds has been presented with a particular focus on the widely used  $U_3Si_2$ . A new interpretation of the irradiation swelling behaviour has been developed with the understanding that  $U_3Si_2$  becomes amorphous during irradiation. Fission gas bubble density and distribution are influenced by fission rate and coalescence and have been shown to change throughout the irradiation period. The fission rate is a major determinant in swelling behaviour; however the changing chemistry of the fuel particle is also believed to exert a strong influence. As a result, the swelling behaviour beyond the knee is understood to be non-linear.

## Acknowledgements

The authors gratefully acknowledge the many persons – fabricators, experimenters, reactor and hot cell personnel, and others – who have contributed to establishing the experiment database on which this study was performed.

## References

- [1] G.L. Hofman, L.A. Neimark, in: Proceedings of the 10th International Meeting on Reduced Enrichment for Research and Test Reactors, Buenos Aires, Argentina, 28 September–1 October 1987, Comision Nacional De Energia Atomica.
- [2] J. Rest, G.L. Hofman, *Fundamental Aspects of Inert Gases in Solids*, Plenum, New York, 1990.
- [3] M.L. Bleiberg, R.M. Berman, B. Lustman, in: Proceedings of the Symposium On Radiation Damage in Solid and Reactor Materials, IAEA, Vienna, 1963, p. 319.
- [4] R.C. Birtcher, J.W. Richardson Jr., M.H. Mueller, *J. Nucl. Mater.* 230 (1996) 158.
- [5] J. Rest, *J. Nucl. Mater.*, doi:10.1016/j.jnucmat.2003.11.008.
- [6] M.L. Bleiberg, L.J. Jones, *Trans. Met. Soc. AIME* 212 (1958) 758.
- [7] J. Bloch, *J. Nucl. Mater.* 6 (1962) 203.
- [8] B. Bethune, *J. Nucl. Mater.* 31 (1969) 197.
- [9] G.L. Hofman, J. Rest, R.C. Birtcher, J.L. Snelgrove, in: Proceedings of the 13th International Meeting on Reduced Enrichment for Research and Test Reactors, Argonne National Laboratory, Report ANL/RERTR/TM-18, 1990.
- [10] J. Rest, G.L. Hofman, *J. Nucl. Mater.* 210 (1994) 187.
- [11] G.L. Hofman, R.F. Domagala, G.L. Copeland, *J. Nucl. Mater.* 150 (1987) 238.
- [12] M.K. Meyer, T.C. Wiencek, S.L. Hayes, G.L. Hofman, *J. Nucl. Mater.* 278 (2000) 358.
- [13] R.L. Senn, Summary Report on the HFED Miniplate Irradiations for the RERTR Program, Oak Ridge National Laboratory, Report ORNL-6539, 1989.
- [14] J.L. Snelgrove, R.F. Domagala, G.L. Hofman, T.C. Wiencek, G.L. Copeland, R.W. Hobbs, R.L. Senn, The Use of  $U_3Si_2$  Dispersed in Aluminium in Plate-Type Fuel Elements for Research and Test Reactors, Argonne National Laboratory, Report ANL/RERTR/TM-11, 1987.
- [15] G.L. Hofman, *J. Nucl. Mater.* 140 (1986) 256.
- [16] J.C. Wood, M.T. Foo, L.C. Berthiaume, in: Proceedings of the 5th International Meeting on Reduced Enrichment for Research and Test Reactors, Argonne National Laboratory, Report ANL/RERTR/TM-4, 1982.
- [17] Safety Evaluation Report related to the Evaluation of Low-Enriched Uranium Silicide-Aluminum Dispersion Fuel for Use in Non-Power Reactors, U.S. Nuclear Regulatory Commission, Report NUREG-1313, 1988.
- [18] D.F. Sears, in: Proceedings of the 13th International Meeting on Reduced Enrichment for Research and Test Reactors, Argonne National Laboratory, Report ANL/RERTR/TM-18, 1990.
- [19] R.T. DeHoff, F.N. Rhines, *Quantitative Microscopy*, McGraw-Hill, New York, 1968.
- [20] G.L. Hofman, J. Rest, J.L. Snelgrove, T. Wiencek, S. Koster van Groos, in: Proceedings of the 19th International Meeting on Reduced Enrichment for Research and Test Reactors, Seoul, Korea, 7–10 October 1996, Korea Atomic Energy Research Institute.
- [21] L. Si DeLuca, H.T. Sumsion, Rate of Growth of Diffusion Layers in U–Al and U–AlSi Couples, Knolls Atomic Power Laboratory, Report KAPL-1747, 1957.